62 carcinogenic (Culp *et al.*, 1998), and high-temperature frying oil fume has been classified into
63 Group 2A (IARC, 2010).

64 Previous PAH exposure studies indicated that the naphthalene was the dominant compound
65 (the breathing zone exposure concentrations= 0.15-0.27 μg m^{-3}) during the beefsteak pan-frying
66 process (Sjaastad *et al.*, 2010). Benzo[a]pyrene concentrations fell to the range of 6-24 ng m^{-3} and
67 150-440 ng m^{-3} for home and commercial kitchens, respectively (Zhu and Wang, 2003).
68 Although many PAH exposure assessment studies have been conducted, most of them were on
69 the cross-sectional basis due to the cost constraints in both samplings and sample analyses.
70 However, considering the chronic health effect of PAHs, the establishment of a long-term
71 exposure data bank is needed for conducting exposure and health risk assessments.

72 To date, mathematical models have been widely used for predicting pollutant concentrations
73 in the industrial hygiene field, particularly both the well-mixed room model and near-field
74 (NF)/far-field (FF) model have been used in indoor environments with known dimensions,
75 ventilation rates, and pollutant generation rates. For example, Nicas *et al.* (2006) used the
76 near-field/far-field model to estimate benzene exposures, and a high R^2 (=0.94) was obtained for
77 predicting exposure of both fields. Gaffney *et al.* (2008) used both well-mixed room model and
78 near-field/far-field model to estimate methanol exposure concentrations in a semiconductor

manufacturing setting, better predictions were obtained from the latter than the former. In principle, if modeling results and measured concentrations had a good correlation, then obtaining a large amount of long-term exposure data might become possible even without conducting field measurements (AIHA, 2009; Kim *et al.*, 2009).

For cooking processes, both the well-mixed room model and near-field/far-field model have never been used for predicting workers' PAH exposures. Though workplace dimensions are usually available, the generated cooking fumes are known inherent with upward thermal drafting forces which might lead to the stratification of pollutant concentrations at different heights (Li and Delsante, 1996). In addition, considering the installation of ventilation (i.e., the exhaust hood), cooking fume emission rates should be replaced by the fugitive emission rates (i.e., should take the capture efficiencies of the exhaust hood into account) before model predictions. Therefore, the feasibility of using both the well-mixed room model and near-field/far-field model for predicting exposures of PAHs emitted from cooking processes is required further investigation.

The present study was conducted in a test room installed with a deep-frying apparatus and an exhaust hood with adjustable ventilation rate for a fixed cooking process (temperature and time, etc.). Emission rates of PAHs were measured, hood capture efficiencies were calculated,

and resultant fugitive emission rates were estimated. Concentrations obtained from both the well-mixed room model and near-field/far-field model were predicted and compared with the measured values. Finally, the feasibilities of both models were assessed, and techniques for predicting exposures of PAHs emitted from cooking processes were proposed. The results obtained from the present study would be helpful for cooking industries to establish long-term PAH exposure data for conducting exposure and health risk assessments.

MATERIALS AND METHODS

Test room and test cooking condition

All experiments were conducted in a test room (L×W×H=3.25m×3.10m×2.75m) with a general kitchen settings (Chiang *et al*., 1998) including an electronic deep-frying machine (2000W, L×W=30cm×15.3cm) (WFT-4L, WISE Inc., Taipei, Taiwan) with a cooking surface 1.1 m above the floor, and a kitchen exhaust hood (L×W=89cm×52cm) (DR-7790ASXL, SAKURA Corp., Taichung, Taiwan) placed at 0.7m above from the deep-frying machine (i.e., 1.8 m above the floor). For each deep-frying test run, it contains 9 repeated cycles, and each cycle includes a 5-min deep-frying period, and followed by a 5-min rest (i.e., the whole test run lasts for 90 minutes). During each deep-frying period, 300g fresh chicken nuggets were deep-fried at 200°C in 3L peanut oil. The cooking oil was repeated used for the whole test run. Three default flow

115 rates of the exhaust hood (i.e., low, medium, and high= 2.64, 3.69, and 5.16 m^3 min^{-1},

116 respectively) were selected in the present study. The only door and window of the test room were

117 closed during the experiment period.

118 ***Sampling for PAH emission rates and exposure concentrations***

119 For each selected ventilation rate, three test runs were conducted to determine its PAH

120 emission rate (G) and resultant exposure concentrations inside the test room. For sampling the

121 emission rate, the test system (including the electronic deep-frying machine and the exhaust hood)

122 was enclosed completely to ensure the non-releasing of emitted PAHs, and a sampling train was

123 placed 15 cm beneath the exhaust hood (Fig. 1), which includes an IOM personal inhalable

124 sampler (Cat. No. 225-70A, SKC Inc., MN, USA) with a quartz fiber filter for collecting

125 particle-phase PAHs, and followed by a XAD-2 tube (Amberlite® XAD®-2, Sigma-Aldrich Corp.,

126 MO, USA) for collecting gas-phase PAHs.

127 Exposure concentrations of PAHs inside the test room were measured using the same

128 sampling train but placed on a mannequin. Samples were collected from both sites of the

129 chef-zone (CZ) (1.5 m in height above the floor, and 0.5 m away from the deep-frying machine to

130 represent the exposure of chefs), and the helper-zone (HZ) (1.5 m in height above the floor, and

131 1.5 m away from the deep-frying machine to represent the exposures of chefs' helpers) (Fig. 2).

PAH analysis

In the present study, each collected filter was microwave extracted using a mixed solvent (n-hexane and dichloromethane, V:V=1:1, 25 mL) for 1 hr. For each collected XAD-2 sample, it was extracted using ultrasonic bath with 2 mL dichloromethane (DCM) for 1 hr (one cycle for 15 min ultrasonic bath followed by 5 min rest, and repeated continuously for 3 cycles). The extracted samples were then concentrated to ~5mL, and cleaned up using the YMC silica gel tube (YMC-DispoPackAT, NH_2 12g, 50μm, YMC CO., LTD., Kyoto, Japan) to ensure no oil was present in the samples. Then, the above samples were re-concentrated and diluted to exactly 1.0mL. The PAH content was determined using a gas chromatograph (GC) (Agilent 7890B, Agilent Technologies Inc., CA, USA) with tandem mass spectrometry (MS/MS) (Agilent 7000C MS/MS Triple Quad, Agilent Technologies Inc., CA, USA) and a computer workstation. This GC/MS/MS was equipped with a Agilent 122-9632 DB-EUPAH column (length 30m × I.D. 0.32mm, film thickness 0.25μm) (Agilent 122-9632 DB-EUPAH, Agilent Technologies Inc., CA, USA) and an Agilent 7693 automatic sampler (Agilent 7693, Agilent Technologies Inc., CA, USA) and was operated under the following conditions: injection volume 10 μL, splitless injection at 310℃, ion sources temperature at 310℃, and oven from 80℃ to 200℃ at 20℃ min^{-1}; 200℃ to 355℃ at 8℃ min^{-1}; hold at 355℃ for 17.325 min. The masses of primary and secondary

149 ions of PAHs were determined with the scan mode for pure PAH standards. Qualification of
150 PAHs was performed using the selected ion monitoring (SIM) mode.

151 The concentrations of 21 PAH species were determined, including naphthalene (Nap),
152 acenaphthylene (AcPy), acenaphthene (Acp), fluorene (Flu), phenanthrene (PA), anthracene
153 (Ant), fluoranthene (FL), pyearene (Pyear), cyclopenta(c,d)pyearene (CYC), benzo(a)anthracene
154 (BaA), chrysene (CHR), benzo(b)fluoranthene (BbF), benzo(k)fluoranthene (BkF),
155 benzo(e)pyearene (BeP), benzo(a)pyearene (BaP), perylene (PER), indeno(1,2,3,-cd)pyearene
156 (IND), dibenzo(a,h)anthracene (DBA), benzo(b)chrycene (BbC), benzo(ghi)perylene (BghiP),
157 and coronene (COR). The GC/MS/MS was calibrated with a diluted standard solution of sixteen
158 PAH compounds (PAH Mixture-610M from Supleco) plus five additional individual PAHs
159 obtained from Merck. Analysis of serial dilutions of PAH standards showed the detection limit of
160 GC/MS/MS falling to the range from 0.06 to 0.45 ppb for the analyzed 21 PAH compounds. Ten
161 consecutive injections of a PAH 610-M standard yielded an average relative standard deviation
162 (RSD) of GC/MS integration area of 3.0 % with a range of 0.8 % to 5.1 %. Quality control (QC)
163 samples adopted the median level of the low calibration curve (30ppb), and were analyzed along
164 with each batch. The QC results were required to fall within ±20% of the calibration curve. To
165 evaluate analytical precision, one spike sample and one random replicate sample were analyzed

for each batch. Recovery efficiencies were determined using a solution containing known PAH concentrations following the same experimental procedures used for the treatment of samples. This study showed recovery efficiencies for the 21 PAH compounds ranging from 65.0% to 117.5%, with an average value of 90.9%. Analysis of field blanks and method blanks, including the glass fiber filter and XAD-2 cartridge, found no significant contamination (GC/MS/MS integrated area < detection limit).

Data analysis

In this study, the total-PAHs concentration was regarded as the sum of the concentrations of 21 PAH compounds for each collected sample. In order to assess the PAH homolog distribution for each collected sample, the total-PAH were further classified into three categories, including the low molecular weight PAHs (LMW-PAHs, containing 2- to 3-ringed PAHs), middle molecular weight PAHs (MMW-PAHs, containing 4-ringed PAHs), and high molecular weight PAHs (HMW-PAHs, containing 5- to 7-ringed PAHs). Moreover, considering that several PAH compounds have been found to be human carcinogens, the carcinogenic potencies associated with PAHs emissions from each emission source were also determined. In principle, the carcinogenic potency of a given PAH compound can be assessed based on its benzo[a]pyearene equivalent concentration (i.e., BaP_{eq}). Calculation of the BaP_{eq} concentration for a given PAH compound

requires the use of the toxic equivalent factor (TEF), which represents the relative carcinogenic potency of the given PAH compound by reference to the specific compound BaP, to adjust its original concentration. To date, several proposals for TEFs (Nisbet and LaGoy, 1992; Malcolm and Dobson, 1994; Larsen and Larsen, 1998) are used in the present study (Table 1). On the basis of this TEF list, the carcinogenic potency of total-PAHs (i.e., total-BaP_{eq}) could be assessed using as the equation 1:

$$Total - BaP_{eq} = \sum_{i=1}^{21} PAH_i \times TEF_i . \quad \text{(Eq. 1)}$$

where, PAH_i and TEF_i are the concentration of the i^{th} PAH compound and its TEF, respectively.

Determining capture efficiencies of the exhaust hood and fugitive emission rates

For the purpose of estimating exposures of cooking workers, PAH emission rates (G) of the investigated cooking process should be replaced by the fugitive emission rates (ER_f). Assuming the capture efficiencies (ε; %) of the exhaust hood is known, then ER_f can be obtained using the following equation:

$$ER_f = G \times (100 - \varepsilon)\%. \quad \text{(Eq. 2)}$$

In principle, the high temperature will lead to a thermal draft with an upward air current during cooking processes. As the heated air rises, it mixes turbulently with the surrounding air. This results in an increasing air plume diameter and volumetric flow rates. The plume flow rate

200 of the thermal draft at the hood entry level can be estimated as the following equation (Popiołek

201 *et al.*, 1998):

202 $Q_p = K_v E^{1/3} (h+Z)^{5/3}$, (Eq. 3)

203 where, Q_p is the plume flow rate at the hood entry level ($m^3 s^{-1}$), E is the heat source power (W), h

204 is the height from the heat source to the hood entry (m), Z is the distance between the heat source

205 and the origin point of the plume (m), and K_v is the coefficient describing the air entrainment by

206 the plume. Here, K_v and Z were as suggested by Yik and Au (2002) to be 0.0065 and 2.25D for

207 cooking processes, respectively. The capture efficiency (ε) of gaseous pollutants emitted from the

208 cooking process can be determined using the equation 4:

209 $$\varepsilon = \frac{q_f}{Q_p} \times 100\% = \frac{q_f}{0.0065E^{1/3}(H+2.25D)^{5/3}} \times 100\% ,$$ (Eq. 4)

210 if $q_f > Q_p$, ε=100%,

211 where, q_f is the exhaust flow rate ($m^3 s^{-1}$). Considering particle phase pollutants emitted from the

212 cooking process were dominated by PM_1, (Lunden *et al.*, 2015) which suggests that their capture

213 efficiencies could also be adopted for gas phase pollutants (i.e., Eq. 4). Therefore, the equation 4

214 was adopted for determining the capture efficiencies (ε) for total-PAHs, gas-phase PAHs,

215 particle-phase PAHs, and total-BaP_{eq} in the present study.

216 ***The selected predicting models***

In the present study, both the well-mixed room model and near-field/far-field model were selected for predicting workers' PAH exposures. Firstly, we assume that fugitive emissions will mixed completely in the kitchen space instantly due to the limited kitchen space and strong mixing effect. Therefore, the obtained fugitive emission rates of PAHs (ER_f) were applied to the well-mixed room model (Reinke and Keil, 2006) to predict the exposures of all workers in the test room (i.e., including chefs and their helpers, and assuming both share the same exposure level) using equation 5:

$$C_{WMR} = \left(C_0 - C_{in} - \frac{ER_f}{Q}\right) e^{\frac{-Q(t-t_0)}{V}} + C_{in} + \frac{ER_f}{Q} \quad , \qquad \text{(Eq. 5)}$$

where, C_{WMR} is the concentration predicted for all workers at time t, C_0 is the concentration of test room at time t_0, C_{in} is the concentration of the inlet air, Q is the inlet air flow rate, and V is the volume of the test room. Secondly, we assume that fugitive emissions will affect more strongly on the exposure of workers who are closer than those of less close to the emission source. In this situation, the obtained fugitive emission rates of PAHs (ER_f) were also applied to the near-field/far-field model (Nicas, 2006) to estimate the exposures of chefs (i.e., near-field exposures) and their helpers (i.e., far-field exposures) using equation 6 and 7, respectively:

$$C_{NF} = \frac{ER_f}{Q} + \frac{ER_f}{\beta} + ER_f \left(\frac{\beta \cdot Q + \lambda_2 \cdot V_N(\beta+Q)}{\beta \cdot Q \cdot V_N(\lambda_1+\lambda_2)}\right) e^{\lambda_1 \cdot t} - ER_f \left(\frac{\beta \cdot Q + \lambda_1 \cdot V_N(\beta+Q)}{\beta \cdot Q \cdot V_N(\lambda_1-\lambda_2)}\right) e^{\lambda_2 \cdot t} \quad , \qquad \text{(Eq. 6)}$$

$$C_{FF} = \frac{ER_f}{Q} + ER_f \left(\frac{\lambda_1 \cdot V_N + \beta}{\beta}\right)\left(\frac{\beta \cdot Q + \lambda_2 \cdot V_N(\beta+Q)}{\beta \cdot Q \cdot V_N(\lambda_1-\lambda_2)}\right) e^{\lambda_1 \cdot t} - ER_f \left(\frac{\lambda_2 \cdot V_N + \beta}{\beta}\right)\left(\frac{\beta \cdot Q + \lambda_1 \cdot V_N(\beta+Q)}{\beta \cdot Q \cdot V_N(\lambda_1-\lambda_2)}\right) e^{\lambda_2 \cdot t} \quad , \qquad \text{(Eq. 7)}$$

where, C_{NF} and C_{FF} are the concentrations predicted respectively for chefs and helpers at time t, V_N and V_F are respectively as the volume of near-field and far-field, β is the air exchange rate between near-field and far-field, and λ_1 and λ_2 respectively represent the air turnover rates of near-field and far-field (in min^{-1}).

RESULTS AND DISCUSSION

PAH emission rates

Table 2 shows the emission rates (or the generation rates) of gas-phase PAHs, particle-phase PAHs, LMW-PAH, MMW-PAH, HMW-PAH and total-BaP_{eq} for the test cooking conditions. Results show that emission rates of the gas-phase PAHs and particle-phase PAHs were 1.45×10^4 ng min^{-1} and 2.14×10^2 ng min^{-1}, respectively. Most generated PAHs were in the form of the gas-phase (98.5%) and were mainly contributed by LMW-PAHs (i.e., PAHs with 2-3 benzene ringed compounds). It is known that PAHs can be generated from cooking processes because of the incomplete combustion or pyrolysis of organic compounds containing hydrogen and carbon. Since temperatures involved in the selected cooking processes is quite low (i.e., 200°C) which can only provide very limited power for the formation of PAHs. Therefore, it is not so surprising to see the dominance of LMW-PAHs (especially naphthalene) in the emitted PAHs. The above inference can also be supported by many cooking-related studies (Schauer *et al.*, 1999, 2002;

253 McDonald *et al.*, 2003; Sjaastad et al., 2010). However, the naphthalene emission rates of the
254 above studies (range= 127-588 μg min^{-1}) were much higher than those found in the present study
255 due to the involved cooking food weights for those of formers (=12.5-68 kg) was much higher
256 than that of the latter (=2.7 kg). The above inference can be further supported by the comparable
257 emission factors obtained from those of the formers (=4.5-16.7 μg min^{-1} kg^{-1}) and the latter (=5.4
258 μg min^{-1} kg^{-1}).

259 For particle-phase PAHs, the emission rates of LMW-, MMW-, and HMW-PAHs were
260 8.97×10^{1}, 1.14×10^{2}, 1.00×10^{1} ng min^{-1}, respectively. PAHs with 3-4 benzene rings (i.e.,
261 MMW-PAHs) were found to be the most dominant compounds, which accounted for 53.38% of
262 article-phase PAHs. Similar results can also be found in other studies (Rogge *et al.*, 1991;
263 McDonald et al., 2003; Saito *et al.*, 2014). They found that particle-phase PAHs contain mainly
264 3-4 ringed compounds, and the two compounds of fluoranthene (FL) and pyrene (Pyr) were
265 found with the highest fractions.

266 Although particle-phase PAHs accounted for only 1.5% of the total-PAH emissions, a higher
267 contribution (=9.5%) to the total-BaP_{eq} emission rates was found in the present study. The above
268 result is not so surprising because MMW- and HMW-PAHs are the most dominant compounds in
269 particle-phase PAHs, and which compounds are known with higher TEFs.

Capture efficiency and fugitive emission rates

For the purpose of estimating cooks' exposures, PAH emission rates (or generation rates, G) should be replaced by fugitive emission rates (ER_f). Therefore, the estimation of hood capture efficiencies (ε) become essential to meet the above purpose. In the present study, the heat source power (E), exhaust flow rate (q_f), exhaust hood height (H), and diameter of the heat source (D, using equivalent surface diameter) were found to be 0.7 m, 2000 W, and 0.242 m, respectively. Based on eq. 4, the capture efficiencies (ε) of the exhaust hood were found to be 39.1%, 54.7%, and 76.5% for three designated exhaust flow rates of 2.64, 3.69, and 5.16 m^3 min^{-1}, respectively. The above captured efficiencies were quite comparable to those obtained from Yik and Au (2002) (i.e., 39%-100%).

The obtained capture efficiencies, together with the obtained emission rates (G) (Table 2) can be used to estimate the fugitive emission rates (ER_f) using eq. 2. The resultant ER_f for the exhaust flow rates (Q) set at 2.64, 3.69, and 5.16 m^3 min^{-1} for total-PAHs were found to be 8.95×10^3, 6.66×10^3, and 3.46×10^3 ng min^{-1}, respectively; gas-phase PAHs were 8.82×10^3, 6.57×10^3, and 3.41×10^3 ng min^{-1}, respectively; particle-phase PAHs were 1.30×10^2, 9.69×10^1, and 5.03×10^1 ng min^{-1}, respectively, and total-BaP_{eq} were 2.26×10^1, 1.68×10^1, and 8.70 ng min^{-1}, respectively. The above results were not so surprising since the increase in the exhaust flow rates (Q) would result

in the increase in the capture efficiencies (ε), which leads to the decrease in the fugitive emission rates (ER_f).

Predicted PAH exposure concentrations

Table 3 shows the predicted PAH exposure concentrations (including gas-phase PAHs, particle-phase PAHs, LMW-PAH, MMW-PAH, HMW-PAH and total-BaP_{eq}) for all workers (i.e., C_{WMR} representing predicted PAH exposure concentrations for workers in both NF and FF), chefs' exposure concentrations (i.e., C_{NF} representing the predicted concentrations for workers in the NF), and helpers' exposure concentrations (i.e., C_{FF} representing the predicted concentrations for workers in the FF) under three designated exhaust hood flow rates (i.e., 2.64 m^3 min^{-1}, 3.69 m^3 min^{-1}, and 5.16 m^3 min^{-1}) using Eq. 5, 6, and 7, respectively. The average random airspeed (β) used in the NF/FF model was measured using an anemometer (TSI 9565-X, TSI Inc., MN, USA) with a thermo-anemometer probe (TSI 966, TSI Inc., MN, USA). In the present study, β was 0.03, 0.03, and 0.04 m s^{-1} when the exhaust hood flow rates were set at 2.64, 3.69, and 5.16 m^3 min^{-1}, respectively. Results show that PAH concentrations (including gas-phase PAHs, particle-phase PAHs, LMW-PAH, MMW-PAH, HMW-PAH and total-BaP_{eq}) in magnitude for the three predicted results were: $C_{NF}>C_{WMR}>C_{FF}$ (Table 3). Since workers in the NF were closer to the emission source than those in FF, the predicted PAH exposure concentrations of C_{NF} and hence

304 were higher than that of C_{FF}. On the other hand, C_{WMR} represents the emitted PAHs being

305 uniformly distributed in the test room, and hence it can be expected that the magnitudes of C_{WMR}

306 fall between C_{NF} and C_{FF}.

307 ***Measured PAH exposure concentrations***

308 Table 4 shows the measured PAH exposure concentrations for all workers (i.e., C_T, including

309 sampling results obtained from both chef-zone (CZ) and helper-zone (HZ)), chef exposure

310 concentrations (i.e., $C_{CZ,}$ sampling results obtained from CZ) and helper exposure concentrations

311 (i.e., C_{HZ}, sampling results obtained from HZ) under three designated exhaust hood flow rate

312 conditions (i.e., 2.64 m^3 min^{-1}, 3.69 m^3 min^{-1}, 5.16 m^3 min^{-1}). Results show that LMW-PAHs

313 dominated in all measured total-PAH concentrations, including C_T, C_{CZ} and C_{HZ}. The above

314 results were consistent with that of fugitive PAH emission results. In particular, most total-PAHs

315 were contributed by the naphthalene (~90%), which was also consistent with the results reported

316 by Sjaastad et al. (2010). Though the measured PAH concentrations for C_{CZ} were slightly higher

317 than that of C_{HZ}, but no significant difference could be found in the present study ($P>0.05$).

318 Therefore, workers in the test kitchen may have very similar PAH exposures regardless of their

319 locations. This could be explained by the circulation of airflow in the test room. In principle,

320 cooking oil fumes could be first lifted by the thermal draft, then partly removed by the exhaust

hood, and the rest reach the ceiling of the kitchen, then turn downward to the floor, and finally combine with the new generated cooking oil fumes, and then repeat the above cycle. As a result, a well-mixed condition was found in the test room which leads to no significant difference in PAH concentration between C_{CZ} and C_{HZ}.

Cionsidering there was no significant difference between the C_{CZ} and C_{HZ}, both results were combined to describe the overall PAH concentrations (C_T) in the test room. For C_T, Table 4 also shows that the mean total-PAHs were increased from1.36×10^2 to 2.93×10^2 ng m^{-3} as exhaust hood flow rates decreased from 5.16 m^3 min^{-1} to 2.64 m^3 min^{-1}. Obviously, the above results can be explained by the fact that the increase in the exhaust hood flow rates would result in the increases in the capture efficiencies.

Table 4 also shows that all measured PAH exposure concentrations (i.e., C_{CZ}, C_{HZ}, and C_T) were ~5 times in magnitude less than the corresponding predicted exposure concentrations (i.e., C_{NF}, C_{FF}, and C_{WMR}). Here, it should be noted that the predictions of C_{NF}, C_{FF}, and C_{WMR} assumes well-mixed in PAH concentrations in the designated zones. However, the thermal draft effect would result in higher concentrations accumulated at the ceiling, and decreased as the height decreased. The above inference is supported by our findings (i.e., C_{CZ}, C_{HZ}, and C_T were much lower than that of the corresponding C_{NF}, C_{FF}, and C_{WMR}). In addition, the stratified concentration

scenario also suggests the concentrations at the same height could be very similar. Since C_{CZ}, C_{HZ}, and C_T were measured at the same height (i.e., 1.5 m in height from the floor), no significant difference in their measured results could be theoretically plausible.

Proposed for predicting workers PAH exposure concentrations

Since the measured PAH concentrations of C_{CZ} and C_{HZ} were not significantly different, the WMR model was selected to serve as a basis for predicting the PAH exposure concentrations. Fig. 3 shows the relationship between WMR model predicted results (i.e., C_{WMR}) and field measured results (i.e., C_T) on the gas-phase PAHs, particle-phase PAHs, total-PAHs, and total-BaP_{eq} basis. High R^2 were consistently found in the gas-phase PAHs, particle-phase PAHs, total-PAHs, and total-BaP_{eq} (= 0.857, 0.711, 0.860, and 0.92, respectively). The above results suggest that the WMR model can be used as a basis for predicting the PAH exposure concentrations of cooking workers.

Comparable R^2 and regression equations were obtained for gas-phase PAHs and total-PAHs, which obviously can be explained by the fact that total-PAHs were dominated by gas-phase PAHs. The particle-phase PAHs were found with the lowest R^2, which indicated that the variation in the particle-phase PAHs was higher than that of others. The regression equation for total-BaP_{eq} concentrations much comparable to that of particle-phase PAHs, rather than gas-phase PAHs. The

355 above results can be explained by the high TEFs assigned for MMW-PAHs and HMW-PAHs (i.e.,
356 main contributors in particle-phase PAHs), and variation of particle-phase PAH was mainly
357 contributed by the LMW-PAHs.

358 Yet, it is true that the resultant regression equations might be not universally applicable. The
359 approach proposed by the present study provides a possibility for establishing a long-term
360 exposure databank for cooking industries for less constraints in both samplings and sample
361 analyses.

362

363 **CONCLUSIONS**

364

365 Most generated PAHs were in the form of the gas-phase and were mainly contributed by
366 LMW-PAHs. Although particle-phase PAHs accounted for a very low fraction of the total-PAH
367 emissions, a higher contribution to the total-BaP_{eq} emission rates was found in the present study.
368 The capture efficiencies of the exhaust hood fall to the range 39.1%- 76.5%, indicating fugitive
369 PAH emission are theoretically plausible. All measured PAH exposure concentrations were ~5
370 times in magnitude less than the corresponding predicted exposure concentrations. Since C_{CZ},
371 C_{HZ}, and C_T were measured at the same height, no significant difference in their measured results
372 could be explained by the circulation effect. On the other hand, C_{CZ}, C_{HZ}, and C_T were much

lower than that of the corresponding C_{NF}, C_{FF}, and C_{WMR}, which suggests that stratified PAH concentrations might be possible in the atmosphere of the test room. The relationship between WMR model predicted results and field measured results was found with high R^2, the above results suggest that the WMR model can be served as a basis for predicting the PAH exposure concentrations of cooking workers. Though the resultant regression equations might not be universally applicable, the present study has proposed a suitable approach for establishing a long-term exposure databank for cooking industries with less constraints in both samplings and sample analyses.

.

ACKOWLEDGMENT

The authors would like to thank Ministry of Science and Technology (MOST) in Taiwan for funding this research work. The co-author Yu-Cheng Chen contributed equivalent to the correspondence author.

REFERENCES

Abdullahi, K.L., Delgado-Saborit, J.M. and Harrison, R.M. (2013). Emissions and indoor concentrations of particulate matter and its specific chemical components from cooking: A review. *Atmos. Environ.* 71: 260-294.

AIHA (2009). *Mathematical models for estimating occupational exposure to chemicals, 2nd deition*. American Industrial Hygiene Association, Washington.

Chiang, T.A., Wu, P.F. and Ko, Y.C. (1998). Prevention of exposure to mutagenic fumes produced by hot cooking oil in taiwanese kitchens. *Environ. Mol. Mutagen.* 31: 92-96.

Culp, S.J., Gaylor, D.W., Sheldon, W.G., Goldstein, L.S. and Beland, F.A. (1998). A comparison of the tumors induced by coal tar and benzo [a] pyrene in a 2-year bioassay. *Carcinogenesis* 19: 117-124.

Gaffney, S., Moody, E., McKinley, M., Knutsen, J., Madl, A. and Paustenbach, D. (2008). Worker exposure to methanol vapors during cleaning of semiconductor wafers in a manufacturing setting. *J. Occup. Environ. Hyg.* 5: 313-324.

Gao, J., Cao, C.-S., Wang, L., Song, T.-H., Zhou, X., Yang, J. and Zhang, X. (2013). Determination of size-dependent source emission rate of cooking-generated aerosol particles at the oilheating stage in an experimental kitchen. *Aerosol Air Qual. Res.* 13: 488-496.

IARC (2010). Household use of solid fuels and high-temperature frying, Cancer, I.A.f.R.o. (Ed.), International Agency for Research on Cancer, Lyon.

Kim, S.Y., Sheppard, L. and Kim, H. (2009). Health effects of long-term air pollution: Influence

409 of exposure prediction methods. *Epidemiology* 20: 442-450.

410 Larsen, J.C. and Larsen, P.B. (1998). Chemical carcinogens: In: Re hester and rm harrison (eds)

411 air pollution and health Cambridge, UK: The Royal Society of Chemistry.

412 Li, C.T., Lin, Y.C., Lee, W.J. and Tsai, P.J. (2003). Emission of polycyclic aromatic hydrocarbons

413 and their carcinogenic potencies from cooking sources to the urban atmosphere. *Environ.*

414 *Health Persp.* 111: 483.

415 Li, Y. and Delsante, A. (1996). Derivation of capture efficiency of kitchen range hoods in a

416 confined space. *Build. Environ.* 31: 461-468.

417 Lunden, M.M., Delp, W.W. and Singer, B.C. (2015). Capture efficiency of cooking-related fine

418 and ultrafine particles by residential exhaust hoods. *Indoor Air* 25: 45-58.

419 Malcolm, H. and Dobson, S. (1994). *The calculation of an environmental assessment level (eal)*

420 *for atmospheric pahs using relative potencies; department of the environment*, London.

421 McDonald, J.D., Zielinska, B., Fujita, E.M., Sagebiel, J.C., Chow, J.C. and Watson, J.G. (2003).

422 Emissions from charbroiling and grilling of chicken and beef. *J. Air Waste Manage* 53:

423 185-194.

424 Mi, H.-H., Liao, W.-T., Chang, H.-C., Chen, S.-J., Lin, C.-C. and Hsieh, L.-T. (2014). Optical

425 emission spectroscopy in cooking exhaust from a wet scrubber/atmospheric plasma

reactor. *Aerosol Air Qual. Res.* 10: 1665-1674.

Nicas, M. (2006). The Near Field/Far Field (Two-Box) Model with a constant contaminant emission rate. In Mathematical models for estimating occupational exposure to chemicals, American Industrial Hygiene Association (AIHA), Fairfax, VA, pp. 47-52..

Nicas, M., Plisko, M.J. and Spencer, J.W. (2006). Estimating benzene exposure at a solvent parts washer. *J. Occup. Environ. Hyg.* 3: 284-291.

Nisbet, I.C. and LaGoy, P.K. (1992). Toxic equivalency factors (tefs) for polycyclic aromatic hydrocarbons (pahs). *Regul. Toxicol. Pharm.* 16: 290-300.

Reinke, P. H. and Keil, C. B. (2006). Well-mixed box model. In Mathematical models for estimating occupational exposure to chemicals, American Industrial Hygiene Association (AIHA), Fairfax, VA, pp. 23-31.

Popiołek, Z., Trzeciakiewicz, Z. and Mierzwinski, S. In (Ed.)^(Eds.) Improvement of a plume volume flux calculation method, International conference on air distribution in rooms, 1998.

Purcaro, G., Navas, J.A., Guardiola, F., Conte, L.S. and Moret, S. (2006). Polycyclic aromatic hydrocarbons in frying oils and snacks. *J. Food Protect.* 69: 199-204.

Rogge, W.F., Hildemann, L.M., Mazurek, M.A., Cass, G.R. and Simoneit, B.R. (1991). Sources

of fine organic aerosol. 1. Charbroilers and meat cooking operations. *Environ. Sci. Technol.* 25: 1112-1125.

Saito, E., Tanaka, N., Miyazaki, A. and Tsuzaki, M. (2014). Concentration and particle size distribution of polycyclic aromatic hydrocarbons formed by thermal cooking. *Food Chem.* 153: 285-291.

Schauer, J.J., Kleeman, M.J., Cass, G.R. and Simoneit, B.R. (1999). Measurement of emissions from air pollution sources. 1. C1 through c29 organic compounds from meat charbroiling. *Environ. Sci. Technol.* 33: 1566-1577.

Schauer, J.J., Kleeman, M.J., Cass, G.R. and Simoneit, B.R. (2002). Measurement of emissions from air pollution sources. 4. C1− c27 organic compounds from cooking with seed oils. *Environ. Sci. Technol.* 36: 567-575.

See, S.W. and Balasubramanian, R. (2006). Physical characteristics of ultrafine particles emitted from different gas cooking methods. *Aerosol Air Qual. Res.* 6: 82-92.

See, S.W. and Balasubramanian, R. (2008). Chemical characteristics of fine particles emitted from different gas cooking methods. *Atmos. Environ.* 42: 8852-8862.

Siegmann, K. and Sattler, K. (1996). Aerosol from hot cooking oil, a possible health hazard. *J. Aerosol Sci.* 27: S493-S494.

460 Sjaastad, A.K., Jørgensen, R.B. and Svendsen, K. (2010). Exposure to polycyclic aromatic
461 hydrocarbons (pahs), mutagenic aldehydes and particulate matter during pan frying of
462 beefsteak. *Occup. Environ. Med.*: oem. 2009.046144.
463 Wang, G., Cheng, S., Wei, W., Wen, W., Wang, X. and Yao, S. (2015). Chemical characteristics of
464 fine particles emitted from different chinese cooking styles. *Aerosol Air Qual. Res.* 15:
465 2357-2366.
466 Yik, F. and Au, P. (2002). Flow rate and capture efficiency of domestic kitchen exhaust hoods for
467 chinese households. *Int. J. Archit. Sci.* 3: 125-134.
468 Zhang, S., Peng, S.-C., Chen, T.-H. and Wang, J.-Z. (2015). Evaluation of inhalation exposure to
469 carcinogenic pm10-bound pahs of people at night markets of an urban area in a
470 metropolis in eastern china. *Aerosol Air Qual. Res.* 15: 1944-1954.
471 Zhu, L.H. and Wang, J. (2003). Sources and patterns of polycyclic aromatic hydrocarbons
472 pollution in kitchen air, china. *Chemosphere* 50: 611-618.
473
474
475

476 **Table Captions**

477 **Table 1.** The studied 21 PAH compounds and their TEFs proposed by Larsen and Larsen (1998),

478 Malcolm and Dobson (1994), Nisbet and LaGoy (1992), and those adopted in the present study.

479 **Table 2.** PAHs emission rates of the gas-phase and particle phase (n=6)

480 **Table 3.** Predicted NF, FF and WMR concentrations (C_{NF}, C_{FF}, and C_{WMR}) of PAHs for the exhaust

481 hood operated under three designated flow rates (Q)

482 **Table 4.** Measured chef, helper and all worker concentrations (C_{CZ}, C_{HZ}, and C_{T}) of PAHs for the

483 exhaust hood operated under three designated flow rates (Q)

484

485

Figure Captions

Fig. 1. Schematic of the site for placing IOM sampler for determining PAH emission rates when the exhaust hood and deep frying machine are in an enclosure condition.

Fig. 2. Schematic of sites for collecting near-field and far-field PAH exposure concentrations

Fig. 3. Relationships between measures (y) and predicted (x) exposure concentrations for (a) gas-phase PAHs, (b) particle-phase PAHs, (c) Total-PAHs, and (d) Total-BaP_{eq} (n=9)

493 **Table 1.** The studied 21 PAH compounds and their TEFs proposed by Larsen and Larsen (1998),
494 Malcolm and Dobson (1994), Nisbet and LaGoy (1992), and those adopted in the present study

PAHs	(Larsen and Larsen, 1998)	(Malcolm and Dobson, 1994)	(Nisbet and LaGoy, 1992)	This study
NaP	-	0.001	0.001	0.001
AcPy	-	0.001	0.001	0.001
Acp	-	0.001	0.001	0.001
Flu	0.05	0.001	0.001	0.05
PA	0.0005	0.001	0.001	0.001
Ant	0.0005	0.01	0.01	0.01
FL	-	0.001	0.001	0.001
Pyr	0.001	0.001	0.001	0.001
BaA	0.005	0.1	0.1	0.1
CHR	0.03	0.01	0.01	0.03
CYC	0.02	0.1	-	0.1
BbF	0.1	0.1	0.1	0.1
BkF	0.1	0.1	0.1	0.1
BeP	0.002	0.001	-	0.002
BaP	1	1	1	1
PER	-	0.001	-	0.001
DBA	1	1	1	1
IND	-	0.1	0.1	0.1
BbC	-	-	-	-[a]
BghiP	0.02	0.01	0.01	0.02
COR	-	0.001	-	0.001

495 [a]No TEF has been suggested.
496

497 **Table 2.** PAHs emission rates of the gas-phase and particle-phase (n=6)

PAHs species	Gas-phase			Particle-phase		
	Mean (ng/min)	SD (ng/min)	Percentage	Mean (ng/min)	SD (ng/min)	Percentage
Naphthalene	1.12×10^{4}	6.68×10^{2}	77.17%	5.10	1.41	2.38%
Acenapthylene	2.08×10^{3}	3.68×10^{2}	14.38%	3.28	9.30×10^{-1}	1.54%
Acenapthene	1.02×10^{2}	2.08×10^{1}	0.71%	8.30×10^{-1}	1.70×10^{-1}	0.39%
Fluorene	3.36×10^{2}	6.50×10^{1}	2.32%	7.10×10^{-1}	4.20×10^{-1}	0.33%
Phenanthrene	4.88×10^{2}	9.03×10^{1}	3.37%	4.62×10^{1}	1.13×10^{1}	21.62%
Anthracene	2.98×10^{2}	6.20×10^{1}	2.06%	3.35×10^{1}	7.49	15.68%
Fluoranthene	ND	--	--	5.77×10^{1}	1.18×10^{1}	27.00%
Pyrene	ND	--	--	4.76×10^{1}	1.01×10^{1}	22.24%
Benzo(a)anthracene	ND	--	--	4.17	8.30×10^{-1}	1.95%
Chrysene	ND	--	--	4.68	9.40×10^{-1}	2.19%
Cyclopenta(c,d)pyrene	ND	--	--	4.25	1.00	1.99%
Benzo(b)fluoranthrene	ND	--	--	1.26	2.60×10^{-1}	0.59%
Benzo(k)fluoranthrene	ND	--	--	8.40×10^{-1}	1.70×10^{-1}	0.39%
Benzo(e)pyrene	ND	--	--	1.02	2.50×10^{-1}	0.48%
Benzo(a)pyrene	ND	--	--	1.76	5.00×10^{-1}	0.82%
Perylene	ND	--	--	ND	--	--
Dibenz(a,h)anthracene	ND	--	--	ND	--	--
Indeno(1,2,3,-cd)pyrene	ND	--	--	ND	--	--
Benzo(b)chrysene	ND	--	--	ND	--	--
Benzo(g,h,i)perylene	ND	--	--	8.90×10^{-1}	1.80×10^{-1}	0.42%
Coronene	ND	--	--	ND	--	--
LMW-PAHs	1.45×10^{4}	9.24×10^{1}	100%	8.97×10^{1}	1.80×10^{1}	41.94%
MMW-PAHs	ND	--	--	1.14×10^{2}	2.35×10^{1}	53.38%
HMW-PAHs	ND	--	--	1.00×10^{1}	2.29	4.68%
Total-PAHs	1.45×10^{4}	1.03×10^{3}	98.55%	2.14×10^{2}	4.35×10^{1}	1.45%
Total-BaP_{eq}	3.36×10^{1}	5.02	90.53%	3.52	8.90×10^{-1}	9.47%

498 ND: non-detected

499

500 **Table 3.** Predicted NF, FF and WMR concentrations (C_{NF}, C_{FF}, and C_{WMR}) of PAHs for the exhaust

501 hood operated under three designated flow rates (Q)

PAHs concentrations (ng/m^3)	Hood exhaust flow rate (Q, m^3/min)								
	2.64			3.69			5.16		
	C_{NF}	C_{FF}	C_{WMR}	C_{NF}	C_{FF}	C_{WMR}	C_{NF}	C_{FF}	C_{WMR}
Gas-phase	2.27×10^{3}	1.50×10^{3}	1.53×10^{3}	1.40×10^{3}	8.26×10^{2}	8.43×10^{2}	5.39×10^{2}	3.14×10^{2}	3.20×10^{2}
Particle-phase	3.35×10^{1}	2.21×10^{1}	2.26×10^{1}	2.07×10^{1}	1.22×10^{1}	1.24×10^{1}	7.95	4.63	4.73
Total-PAHs	2.33×10^{3}	1.54×10^{3}	1.57×10^{3}	1.43×10^{3}	8.44×10^{2}	8.55×10^{2}	5.47×10^{2}	3.19×10^{2}	3.25×10^{2}
Total-BaP_{eq}	5.83	3.85	3.92	3.60	2.12	2.16	1.38	8.10×10^{-1}	8.20×10^{-1}

502

503 **Table 4.** Measured chef, helper and all worker concentrations (C_{CZ}, C_{HZ}, and C_T) of PAHs for the
504 exhaust hood operated under three designated flow rates (Q)

Hood exhaust flow rate (Q, m^3/min)	PAHs concentrations (ng/m^3)	LMW-PAHs	MMW-PAHs	HMW-PAHs	Total-PAHs	Total-BaP_{eq}
2.64 (n=3)	C_{CZ}	2.92×10^{2}	1.97	9.65×10^{-1}	2.95×10^{2}	7.90×10^{-1}
	SD	1.42×10^{1}	8.80×10^{-1}	4.30×10^{-1}	1.45×10^{1}	1.10×10^{-1}
	C_{HZ}	2.89×10^{2}	1.25	6.75×10^{-1}	2.91×10^{2}	7.47×10^{-1}
	SD	3.08×10^{1}	5.20×10^{-1}	2.80×10^{-1}	3.11×10^{1}	9.00×10^{-2}
	C_T	2.90×10^{2}	1.61	8.20×10^{-1}	2.93×10^{2}	7.64×10^{-1}
	SD	2.11×10^{1}	6.20×10^{-1}	3.20×10^{-1}	2.11×10^{1}	9.00×10^{-2}
3.69 (n=3)	C_{CZ}	1.61×10^{2}	8.03×10^{-1}	4.78×10^{-1}	1.62×10^{2}	5.20×10^{-1}
	SD	3.10×10^{1}	2.40×10^{-1}	1.40×10^{-1}	3.07×10^{1}	5.00×10^{-2}
	C_{HZ}	1.52×10^{2}	1.04	5.34×10^{-1}	1.54×10^{2}	5.87×10^{-1}
	SD	1.95×10^{1}	1.60×10^{-1}	8.00×10^{-2}	1.93×10^{1}	7.00×10^{-2}
	C_T	1.57×10^{2}	9.19×10^{-1}	5.06×10^{-1}	1.58×10^{2}	5.51×10^{-1}
	SD	2.53×10^{1}	2.00×10^{-1}	1.10×10^{-1}	2.50×10^{1}	5.00×10^{-2}
5.16 (n=3)	C_{CZ}	1.40×10^{2}	7.28×10^{-1}	3.85×10^{-1}	1.41×10^{2}	3.59×10^{-1}
	SD	1.37×10^{1}	2.00×10^{-1}	1.10×10^{-1}	1.34×10^{1}	1.00×10^{-2}
	C_{HZ}	1.30×10^{2}	7.00×10^{-1}	3.54×10^{-1}	1.31×10^{2}	3.45×10^{-1}
	SD	2.53×10^{1}	2.40×10^{-1}	1.20×10^{-1}	2.56×10^{1}	1.20×10^{-1}
	C_T	1.35×10^{2}	7.14×10^{-1}	3.70×10^{-1}	1.36×10^{2}	3.52×10^{-1}
	SD	1.01×10^{1}	2.20×10^{-1}	1.10×10^{-1}	1.02×10^{1}	6.00×10^{-2}

505

506

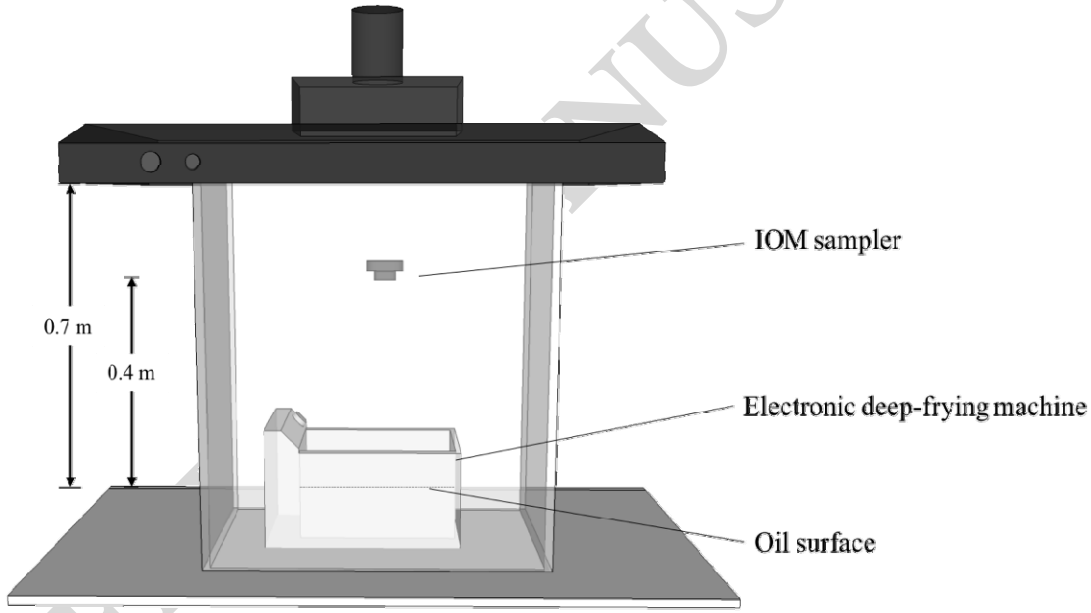

Fig. 1

507

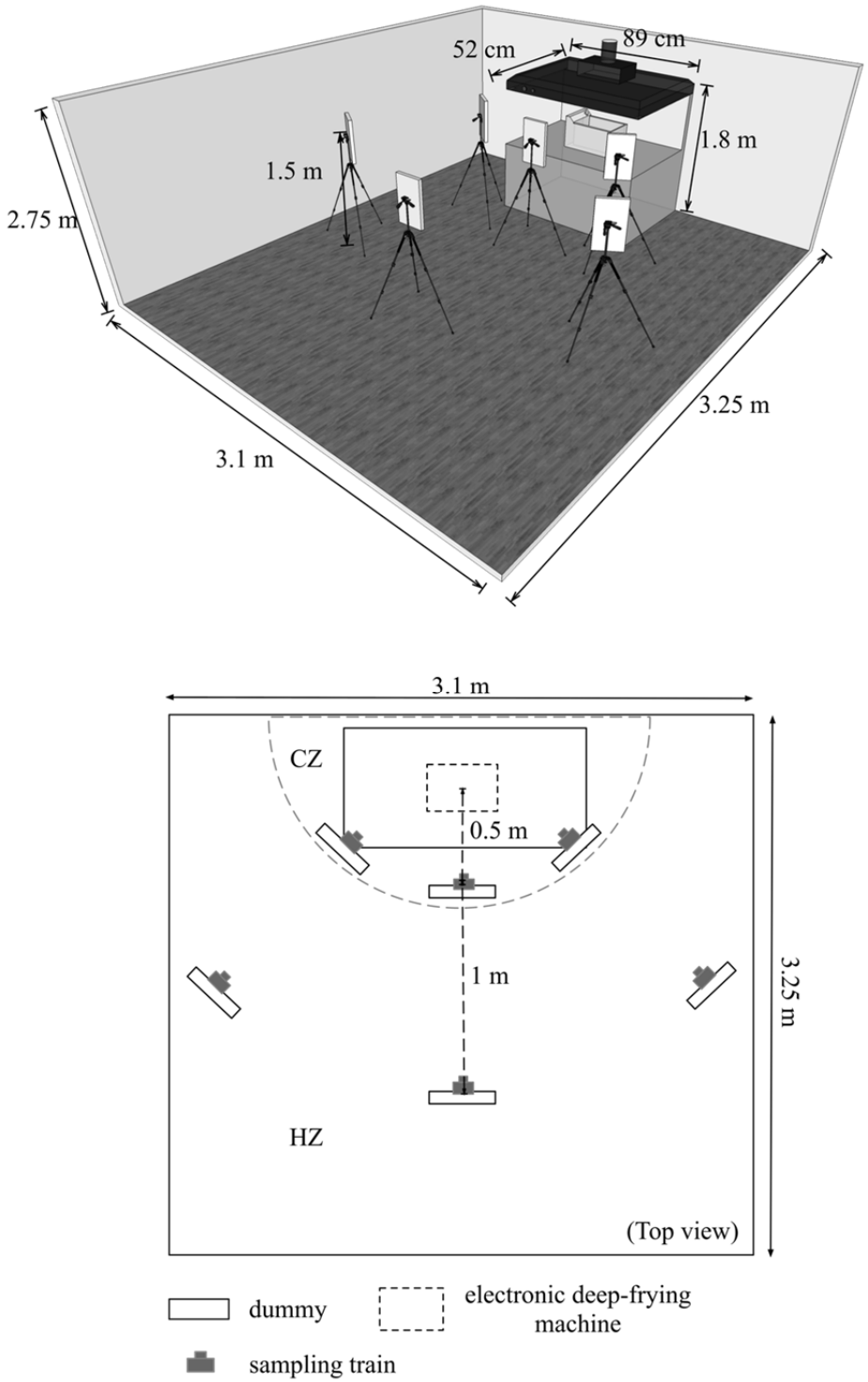
52 cm
89 cm
1.8 m
1.5 m
2.75 m
3.25 m
3.1 m
3.1 m
CZ
0.5 m
1 m
3.25 m
HZ
(Top view)
dummy
electronic deep-frying machine
sampling train

Fig. 2.

508

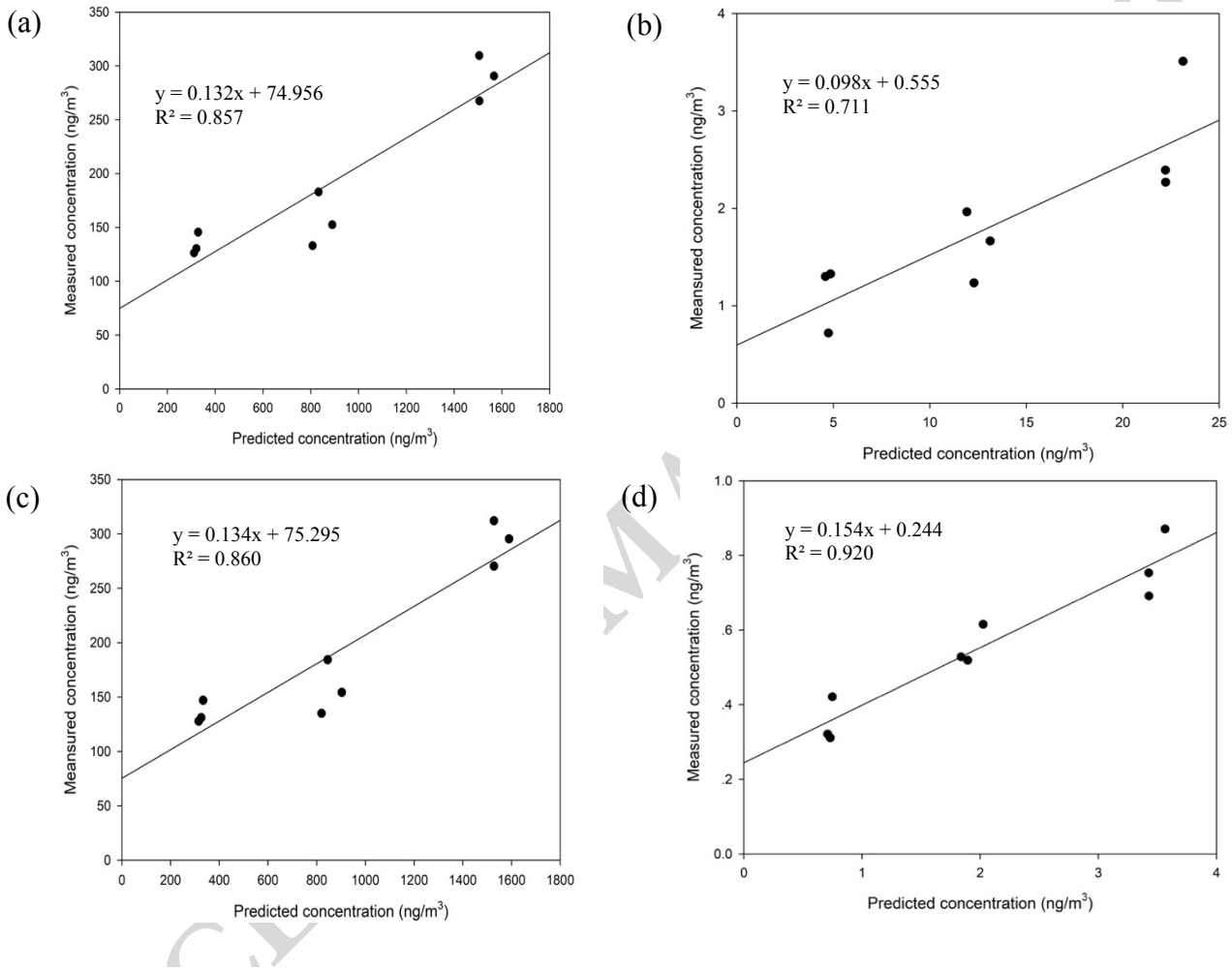
(a)
y = 0.132x + 74.956
R² = 0.857
Measured concentration (ng/m3)
Predicted concentration (ng/m3)
(b)
y = 0.098x + 0.555
R² = 0.711
Meansured concentration (ng/m3)
Predicted concentration (ng/m3)
(c)
y = 0.134x + 75.295
R² = 0.860
Meansured concentration (ng/m3)
Predicted concentration (ng/m3)
(d)
y = 0.154x + 0.244
R² = 0.920
Measured concentration (ng/m3)
Predicted concentration (ng/m3)

Fig. 3.